Int. J. Electrochem. Sci., 17 **(2022)** Article Number: 220349, doi: 10.20964/2022.03.48

International Journal of
ELECTROCHEMICAL
SCIENCE
www.electrochemsci.org

Mathematical Modeling of pH-Based Potentiometric Biosensor Using Akbari-Ganji Method

R. Shanthi[1], *M. Chitra Devi*[2], *Marwan Abukhaled*[3], *Michael E.G. Lyons*[4], *L. Rajendran*[1,*]

[1] Department of Mathematics, AMET (Deemed to be University), Kanathur, Chennai, India
[2] Department of Mathematics, Anna University, University College of Engineering, Dindigul, India.
[3] Department of Mathematics and Statistics, American University of Sharjah, Sharjah, UAE
[4] School of Chemistry & AMBER National Centre, University of Dublin, Trinity College Dublin, Dublin 2, Ireland
[*]E-mail: raj_sms@rediffmail.com

Received: 8 December 2021 / *Accepted:* 22 January 2022 / *Published:* 2 February 2022

This study discusses a mathematical model for the steady-state reaction of a pH-based potentiometric biosensor immobilizing organophosphorus hydrolase (OPH). The model that combines diffusion and enzymatic reaction processes in the membrane is a system of five interconnected nonlinear reaction-diffusion equations. Approximate analytical expressions for the substrate concentration (organophosphorus pesticides (OPs)) and products are derived for all possible values of Thiele modulus and buffer concentration using the Akbari-Ganji method. In addition, analytical expressions for the current, sensitivity, and resistance of pH-based potentiometric biosensors are also derived. The obtained analytical results are convergent on the prescribed domain and firmly match the fourth-order Runge-Kutta numerical simulations.

Keywords: Mathematical modeling, reaction-diffusion, pH-based potentiometric biosensor, Akbari-Ganji method, nonlinear equations.

1. INTRODUCTION

Enzymes are deemed the most suitable recognition elements owing to their high chemical specificity and intrinsic biocatalytic signal amplification. Biosensors use enzymes, which catalyze the interaction with an analyte are now possible due to advances in biological components and microsystem technology. Biosensors can be classified according to the mode of physicochemical transduction or the type of biorecognition element.

Organophosphorus pesticides (Ops) are evaluated using enzyme-based electrochemical biosensors [1-5]. In biosensors for determining OPs, organophosphorus hydrolase (OPH) has recently

been used instead of acetylcholinesterase (AChE) or butyrylcholinesterase (BChE). With the discovery of organophosphorus hydrolase (OPH), an enzyme that can hydrolyze a wide range of organophosphate pesticides releasing detectable products [6,7], several enzymes and microbial biosensors based on OPH for rapid, simple, selective monitoring of these neurotoxic pesticides with the potential for in the field analysis have been reported [8-12]. Many experimental methods for determining organophosphorus pesticides have been reported in gas and liquid chromatographic technologies [13], immunoassays [14], and inhibition of cholinesterase [15].

Modeling OPH biosensors is crucial to understanding their behavior, analyzing their analytical characteristics, and optimizing industrial processes. Examples of non-OPH models of pH-based potentiometric enzyme electrodes immobilizing include the use of magnetic polysiloxane polyvinyl alcohol particles [16] and a model for a pH-based enzymatically coupled field-effect transistor [17]. Lihong et al. have presented a numerical solution for estimating the steady-state response of pH-based potentiometric biosensors that immobilize organophosphorus hydrolase (OPH) [1]. Meena et al. [18] discussed a model of a pH-based potentiometric biosensor immobilizing organophosphorus hydrolase. Saranya et al. [19] utilized a modified homotopy perturbation method to derive semi-analytical expressions for the substrate and product concentrations.

In this communication, we present a simple approximate closed-form formula for the concentrations of the substrate (organophosphorus pesticides (OPs)) and deprotonation products for all values of the system parameters using the efficient AGM method. pH-based potentiometric biosensors' current, sensitivity, and resistance are also presented and discussed for various experimental parameters.

2. FORMULATION AND SOLUTION OF THE MODEL

Figure 1 shows a schematic diagram of a pH-based potentiometric biosensor that immobilises organophosphorus hydrolase (OPH). S is the organophosphorus chemicals' substrate in this diagram (OPs). The hydrolysis products of organ phosphodiester and alcohol, respectively, are P_hH and ZH.

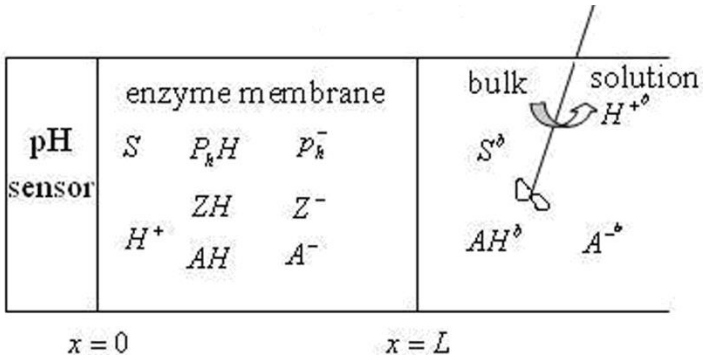

Figure 1. Schematic representation of pH-based potentiometric biosensor immobilizing OPH.

In Figure 1, AH is the added external buffer and P_h^-, Z^-, A^-, and H^+ are the deprotonation products. Within the enzyme membrane, an enzyme-catalyzed reaction is described by:

$$S \xrightarrow[H_2O]{E} P_hH + ZH, \qquad P_hH \underset{k_p'}{\overset{k_p}{\Leftrightarrow}} P_h^- + H^-, \qquad ZH \underset{k_Z'}{\overset{k_Z}{\Leftrightarrow}} Z^- + H^+, \qquad AH \underset{k_A'}{\overset{k_A}{\Leftrightarrow}} A^- + H^+. \tag{1}$$

2.1. Mathematical formulation of the probelm

We begin by assuming that [1]: First, the sensor surface is of infinite extent and the concentrations vary in the dimension that is normal to the surface; second, the surface is impassable to the substrate and the products; third, the stirring rate is sufficiently high to ensure that the concentrations at the interface of the membrane and bulk solutions are equal; fourth, only diffusion is the transport median inside the membrane, and the concentrations of the formed products are negligible in the bulk solution, and fifth, all species' diffusion coefficients are equal. The governing diffusion-reaction equation is given by

$$\frac{\partial C_i}{\partial t} = D_i \frac{\partial^2 C_i}{\partial x^2} + R(C_i), \tag{1}$$

where C_i is the species concentration, D_i is the diffusion coefficients, and R is the nonlinear reaction rate. The diffusion-reaction equations in steady-state are [1]:

$$D\frac{d^2[S]}{dx^2} - R = 0, \tag{2}$$

$$D\frac{d^2[P_hH]}{dx^2} + R - r_{P_hH} = 0, \tag{3}$$

$$D\frac{d^2[P_h^-]}{dx^2} + r_{P_hH} = 0, \tag{4}$$

$$D\frac{d^2[ZH]}{dx^2} + R - r_{ZH} = 0, \tag{5}$$

$$D\frac{d^2[Z^-]}{dx^2} + r_{ZH} = 0, \tag{6}$$

$$D\frac{d^2[AH]}{dx^2} - r_{AH} = 0, \tag{7}$$

$$D\frac{d^2[A^-]}{dx^2} + r_{AH} = 0, \tag{8}$$

$$D\frac{d^2[H^+]}{dx^2} + r_{P_hH} + r_{ZH} + r_{AH} = 0, \tag{9}$$

where R, r_{P_hH}, r_{ZH}, and r_{AH} are the reaction rates for the reactions in (1). It is also assumed that the substrate S follows the catalysts via Michaelis-Menten kinetics as per the scheme:

$$S + EH^- \underset{k_{-1}}{\overset{k_1}{\leftrightarrow}} EH^- - S \xrightarrow{k_2} EH^- - P \xrightarrow{k_3} E + P. \tag{10}$$

The overall rate R is given by

$$R = \frac{V_{max}[S]}{[S] + k_m}, \tag{11}$$

where $V_{max} = \frac{k_2 k_3 [E]_t}{(k_2 + k_3)}$, $k_m = \frac{(k_2 + k_{-1})}{(k_2 + k_3)} \frac{k_3}{k_1}$ in which k_1 and k_{-1} are the rate constants for the Michaelis complex formation, k_2 is the chemical transformation rate constant, k_3 is the product dissociation rate

constant, and $[\mathrm{E}]_t$ is the enzyme concentration. We introduce the following set of dimensionless variables:

$$\overline{C_{\mathrm{i}}} = \frac{C_{\mathrm{i}}}{K_m},\ \overline{C_{\mathrm{i}}^{b}} = \frac{C_{\mathrm{i}}^{b}}{K_m}\ \overline{x} = \frac{x}{L}\text{, and } a^2 = \frac{L^2 V_{\max}}{DK_m}, \tag{12}$$

where K_m is the Michaelis-Menten constant. We define the composite species as follows [1]

$$[\mathrm{P_h}]_{\mathrm{T}} = [\mathrm{P_hH}] + [\mathrm{P_h^-}]\text{, } [\mathrm{Z}]_{\mathrm{T}} = [\mathrm{ZH}] + [\mathrm{Z^-}]\text{, } [\mathrm{A}]_{\mathrm{T}} = [\mathrm{AH}] + [\mathrm{A^-}]\text{,}$$
$$[\mathrm{H^+}]_{\mathrm{T}} = [\mathrm{H^+}] + [\mathrm{P_hH}] + [\mathrm{ZH}] + [\mathrm{AH}], \tag{13}$$

where $[\mathrm{P_h}]_{\mathrm{T}}$, $[\mathrm{Z}]_{\mathrm{T}}$ and $[A]_T$ represent the sums of dissociated and undissociated concentrations of the species $\mathrm{P_hH}$, ZH, and AH, respectively. The instantaneous reaction terms $r_{\mathrm{P_hH}}, r_{\mathrm{ZH}}, r_{\mathrm{AH}}, r_{\mathrm{AH}}$ are cancelled as per Eq. (14). From Eq. (14) and the dimensionless variables in Eq. (13), the nonlinear system (3)-(9) is converted into the following dimensionless nonlinear boundary value system

$$\frac{d^2\,\overline{[\mathrm{S}]}}{d\overline{x}^2} - a^2\frac{\overline{[\mathrm{S}]}}{\overline{[\mathrm{S}]}+1} = 0, \tag{14}$$

$$\frac{d^2\,\overline{[P_h]_T}}{d\overline{x}^2} + a^2\frac{\overline{[\mathrm{S}]}}{\overline{[\mathrm{S}]}+1} = 0, \tag{15}$$

$$\frac{d^2\,\overline{[\mathrm{Z}]_{\mathrm{T}}}}{d\overline{x}^2} + a^2\frac{\overline{[\mathrm{S}]}}{\overline{[\mathrm{S}]}+1} = 0, \tag{16}$$

$$\frac{d^2\,\overline{[\mathrm{A}]_{\mathrm{T}}}}{d\overline{x}^2} = 0, \tag{17}$$

$$\frac{d^2\,\overline{[\mathrm{H^+}]_{\mathrm{T}}}}{d\overline{x}^2} + 2a^2\frac{\overline{[\mathrm{S}]}}{\overline{[\mathrm{S}]}+1} = 0, \tag{18}$$

where a is the Thiele modulus. The dimensionless boundary conditions become

$$\frac{d\overline{C_{\mathrm{i}}}}{d\overline{x}}(0) = 0;\ \text{for } \overline{C_{\mathrm{i}}} = \overline{[\mathrm{S}]},\ \overline{[\mathrm{P_h}]_{\mathrm{T}}},\ \overline{[\mathrm{Z}]_{\mathrm{T}}},\ \overline{[\mathrm{A}]_{\mathrm{T}}},\ \overline{[\mathrm{H^+}]_{\mathrm{T}}}\text{,} \tag{19}$$

$$\overline{C_{\mathrm{i}}}(1) = \overline{C_{\mathrm{i}}^{b}};\ \text{for } \overline{C_{\mathrm{i}}} = \overline{[\mathrm{S}]}, \overline{[\mathrm{A}]_{\mathrm{T}}},\ \overline{[\mathrm{H^+}]_{\mathrm{T}}};\ \ \overline{[\mathrm{P_h}]_{\mathrm{T}}}(1) = \overline{[\mathrm{Z}]_{\mathrm{T}}}(1) = 0. \tag{20}$$

From Eqs. (15)-(17) and Eq. (19), we have

$$\frac{d^2\,\overline{[\mathrm{P_h}]_{\mathrm{T}}}}{d\overline{x}^2} = \frac{d^2\,\overline{[\mathrm{Z}]_{\mathrm{T}}}}{d\overline{x}^2} = \frac{1}{2}\frac{d\,\overline{[\mathrm{H^+}]_{\mathrm{T}}}}{d\overline{x}^2} = -\frac{d^2\,\overline{[\mathrm{S}]}}{d\overline{x}^2}, \tag{21}$$

for which the solution, obtained by direct integration, is given by

$$\overline{[\mathrm{P_h}]_{\mathrm{T}}}(\overline{x}) = \overline{[\mathrm{Z}]_{\mathrm{T}}}(\overline{x}) = \frac{1}{2}\,\overline{[\mathrm{H^+}]_{\mathrm{T}}}(\overline{x}) = -\,\overline{[\mathrm{S}]} + C_1\overline{x} + C_2. \tag{22}$$

Using boundary conditions (20) and (21) in Eq. (23), we obtain the following concentrations:

$$\overline{[\mathrm{P_h}]_{\mathrm{T}}}(\overline{x}) = \overline{[\mathrm{Z}]_{\mathrm{T}}}(\overline{x}) = -\,\overline{[\mathrm{S}]} + \overline{[\mathrm{S}]}^{b},\qquad \overline{[\mathrm{H^+}]_{\mathrm{T}}}(\overline{x}) = 2\left(-\,\overline{[\mathrm{S}]} + \overline{[\mathrm{S}]}^{b}\right) + \overline{[\mathrm{H^+}]_{\mathrm{T}}}^{\mathrm{b}}. \tag{23}$$

Similarly, by direct integration of Eq. (18) and the use of the boundary conditions, we obtain

$$\overline{[\mathrm{A}]_{\mathrm{T}}}(\overline{x}) = \overline{[\mathrm{A}]_{\mathrm{T}}}^{\mathrm{b}}. \tag{24}$$

The dimensionless current is then reduced to

$$\psi = \frac{I}{n_e FD}\left[\frac{L}{[\mathrm{S}]^{\mathrm{b}}}\right] = \left.\frac{d\,\overline{[\mathrm{P_h}]_{\mathrm{T}}}}{d\overline{x}}\right|_{\overline{x}=1}. \tag{25}$$

2.2. Analytical expressions of the concentrations using Akbari-Ganji method

Although many numerical solutions are accurate and efficient to obtain approximate solutions of nonlinear systems, some of their downsides are more serious about being ignored. Numerical stability and adjusting parameters to match the numerical data can be tremendously challenging to realize numerical solutions. Therefore, analytical solutions are more preferred by researchers as they give a better insight for analyzing the effect of model parameters. Over the past four decades, many reliable and highly accurate analytical methods have emerged and been successfully utilized in solving many nonlinear models in various fields of science. To list a few, we mention the homotopy analysis [20, 21], variational iteration [22, 23], differential transformation [24], Adomian decomposition [25], Green's function-fixed point [26, 27], homotopy perturbation (HPM) [28-31], Taylor series [32-36], and Akbari-Ganji method [37-41].

In this article, we used the Akbari-Ganji method to derive the following formula for the concentration of substrate (see Appendix-A for details):

$$\overline{[\mathrm{S}]}(\overline{x}) = \overline{[\mathrm{S}]}^{b}\,\frac{\cosh\,(m\overline{x})}{\cosh\,m}, \tag{26}$$

where

$$m = \frac{a}{\sqrt{1+\overline{[\mathrm{S}]}^{b}}}. \tag{27}$$

Substituting Eq. (27) into Eq. (24) yields the following approximate analytical expressions for the concentrations of $\overline{[\mathrm{P_h}]_\mathrm{T}}$, $\overline{[\mathrm{Z}]_\mathrm{T}}$ and $\overline{[\mathrm{H^+}]_\mathrm{T}}$:

$$\overline{[\mathrm{P_h}]_\mathrm{T}}(\overline{x}) = \overline{[\mathrm{Z}]_\mathrm{T}}(\overline{x}) = \overline{[\mathrm{S}]}^{b}\left(1-\frac{\cosh\,(m\overline{x})}{\cosh\,m}\right), \tag{28}$$

$$\overline{[\mathrm{H^+}]_\mathrm{T}}(\overline{x}) = 2\overline{[\mathrm{S}]}^{b}\left(1-\frac{\cosh\,(m\overline{x})}{\cosh\,m}\right) + \overline{[\mathrm{H^+}]_\mathrm{T}}^{\mathrm{b}}. \tag{29}$$

The dimensionless current is then readily obtained

$$\psi = \frac{I}{n_e F D}\left[\frac{L}{K_m}\right] = \left.\frac{\mathrm{d}\,\overline{[\mathrm{P_h}]_\mathrm{T}}}{\mathrm{d}\overline{x}}\right|_{\overline{x}=1} = -\overline{[\mathrm{S}]}^{b}\,m\tanh m, \tag{30}$$

The current in dimensionless form is computed by the formula:

$$\frac{I}{n_e F} = -\frac{D[\mathrm{S}]^{b}}{LK_m}\,m\tanh m, \tag{31}$$

$$m = \frac{a}{\sqrt{1+\overline{[\mathrm{S}]}^{b}}} = \sqrt{\frac{V_{\max}\,L^2}{D(K_m+\,[\mathrm{S}]^{\mathrm{b}})}}. \tag{32}$$

3. RESULTS AND DISCUSSION

Meena et al. [18] employed a modified version of the homotopy perturbation method (HPM) to derive the following approximate expression for the substrate concentration:

$$\overline{[S]}(\overline{x}) = \frac{\overline{[S]}^{b}(e^{a\overline{x}} + e^{-a\overline{x}})}{(e^{a} + e^{-a})} - \frac{(\overline{[S]}^{b})^{2}}{(e^{a} + e^{-a})^{2}}\left[2 - \frac{(e^{2a\overline{x}} + e^{-2a\overline{x}})}{3}\right]\left[e^{a\overline{x}} + e^{-a\overline{x}} - e^{a} - e^{-a}\right] \quad (33)$$

Tables 1 and 2 give a comparison between the proposed AGM solution given in Eq. (27), the HPM solution given in Eq. (34), and a numerical solution obtained by MATLAB function pdex4 (see Appendix B).

Table 1. Comparison of analytical expression of dimensionless concentration $\overline{[S]}(\overline{x})$ with simulation result for various values of a when $\overline{[S]}^{b} = 1$.

$\overline{x}$	$\overline{[S]}^{b} = 1, a = 0.1$					$\overline{[S]}^{b} = 1, a = 0.5$					$\overline{[S]}^{b} = 1, a = 1$				
	Numerical	HPM Eq.(34)	AGM Eq.(27)	% deviation		Numerical	HPM Eq.(34)	AGM Eq.(27)	% deviation		Numerical	HPM Eq.(34)	AGM Eq.(27)	% deviation	
				Eq.(34)	Eq.(27)				Eq.(34)	Eq.(27)				Eq.(34)	Eq.(27)
0.0	0.9975	0.9983	0.9975	0.0802	0.0000	0.9391	0.9537	0.9406	1.5547	0.1597	0.7760	0.8001	0.7933	3.1057	2.2294
0.2	0.9976	0.9984	0.9976	0.0802	0.0000	0.9416	0.9549	0.9430	1.4125	0.1487	0.7847	0.8016	0.8012	2.1537	2.1027
0.4	0.9979	0.9986	0.9979	0.0701	0.0000	0.9488	0.9587	0.9500	1.0434	0.1265	0.8111	0.8081	0.8252	0.3699	1.7384
0.6	0.9984	0.9989	0.9984	0.0501	0.0000	0.9610	0.9662	0.9618	0.5411	0.0832	0.8553	0.8278	0.8658	3.2152	1.2276
0.8	0.9991	0.9994	0.9991	0.0300	0.0000	0.9780	0.9790	0.9785	0.1022	0.0511	0.9181	0.8789	0.9236	4.2697	0.5991
1.0	1.0000	1.0000	1.0000	0.0000	0.0000	1.0000	1.0000	1.0000	0.0000	0.0000	1.0000	1.0000	1.0000	0.0000	0.0000
	Average deviation			0.0518	0.0000	Average deviation			0.7757	0.0949	Average deviation			2.1857	1.3162

Table 2. Comparison of analytical expression of dimensionless concentration $\overline{[S]}(\overline{x})$ with simulation result for various values of $\overline{[S]}^{b}$ when $a = 0.1$.

$\overline{x}$	$\overline{[S]}^{b} = 0.1, a = 0.1$					$\overline{[S]}^{b} = 5, a = 0.1$					$\overline{[S]}^{b} = 10, a = 0.1$				
	Numerical	HPM Eq.(34)	AGM Eq.(27)	% deviation		Numerical	HPM Eq.(34)	AGM Eq.(27)	% deviation		Numerical	HPM Eq.(34)	AGM Eq.(27)	% deviation	
				Eq.(34)	Eq.(27)				Eq.(34)	Eq.(27)				Eq.(34)	Eq.(27)
0.0	0.0995	0.0995	0.0995	0.0000	0.0000	4.9958	5.0577	4.9958	1.2390	0.0000	9.9955	10.2805	9.9955	2.8513	0.0000
0.2	0.0996	0.0995	0.0995	0.1004	0.1004	4.996	5.0577	4.9958	1.2350	0.0040	9.9956	10.2805	9.9955	2.8503	0.0010
0.4	0.0996	0.0996	0.0996	0.0000	0.0000	4.9965	5.0553	4.996	1.1768	0.0100	9.9962	10.2692	9.9956	2.7310	0.0060
0.6	0.0997	0.0996	0.0996	0.1003	0.1003	4.9973	5.0483	4.9965	1.0206	0.0160	9.9971	10.2352	9.9962	2.3817	0.0090
0.8	0.0998	0.0997	0.0997	0.1002	0.1002	4.9985	5.0367	4.9973	0.7642	0.0240	9.9984	10.1788	9.9971	1.8043	0.0130
1.0	0.1000	0.0998	0.0998	0.2000	0.2000	5	5.0206	4.9985	0.4120	0.0300	10	10.1003	9.9984	1.0030	0.0160
	Average deviation			0.0835	0.0835	Average deviation			0.9746	0.0140	Average deviation			2.2703	0.0075

Tables 1 and 2 show that the maximum error for the AGM method is 1.3162% and for HPM is 2.2703%. Therefore, the accuracy of the proposed method surpasses the accuracy of the HPM. In addition, the approximate solution obtained using the AGM method archives all the parameters in the

equations immediately. In contrast, the homotopy perturbation method needed two iterations to approximate all parameters' approximate solution to appear in the differential equation.

In the following subsections, we study the sensitivity and resistance of biosensors [42-45] using these derived concentrations and current expressions.

3.1. Sensitivity of biosensor

The amperometric biosensor sensitivity, denoted by B_S, is defined as the maximal biosensor current density gradient to the substrate concentration $[S]^b$ [45]. Therefore, $[S]^b$ is computed by

$$B_S([S]^b) = \frac{[S]^b}{I([S]^b)} \frac{dI([S]^b)}{d[S]^b} = 1 - \frac{[S]^b}{2(K_m + [S]^b)} \left(1 + m(\coth(m) - \tanh(m))\right), \quad (34)$$

where $I([S]^b)$ is the steady-state biosensor current density. From Eq.(35), it is deduced that the sensitivity B_S varies between 0 and 1.

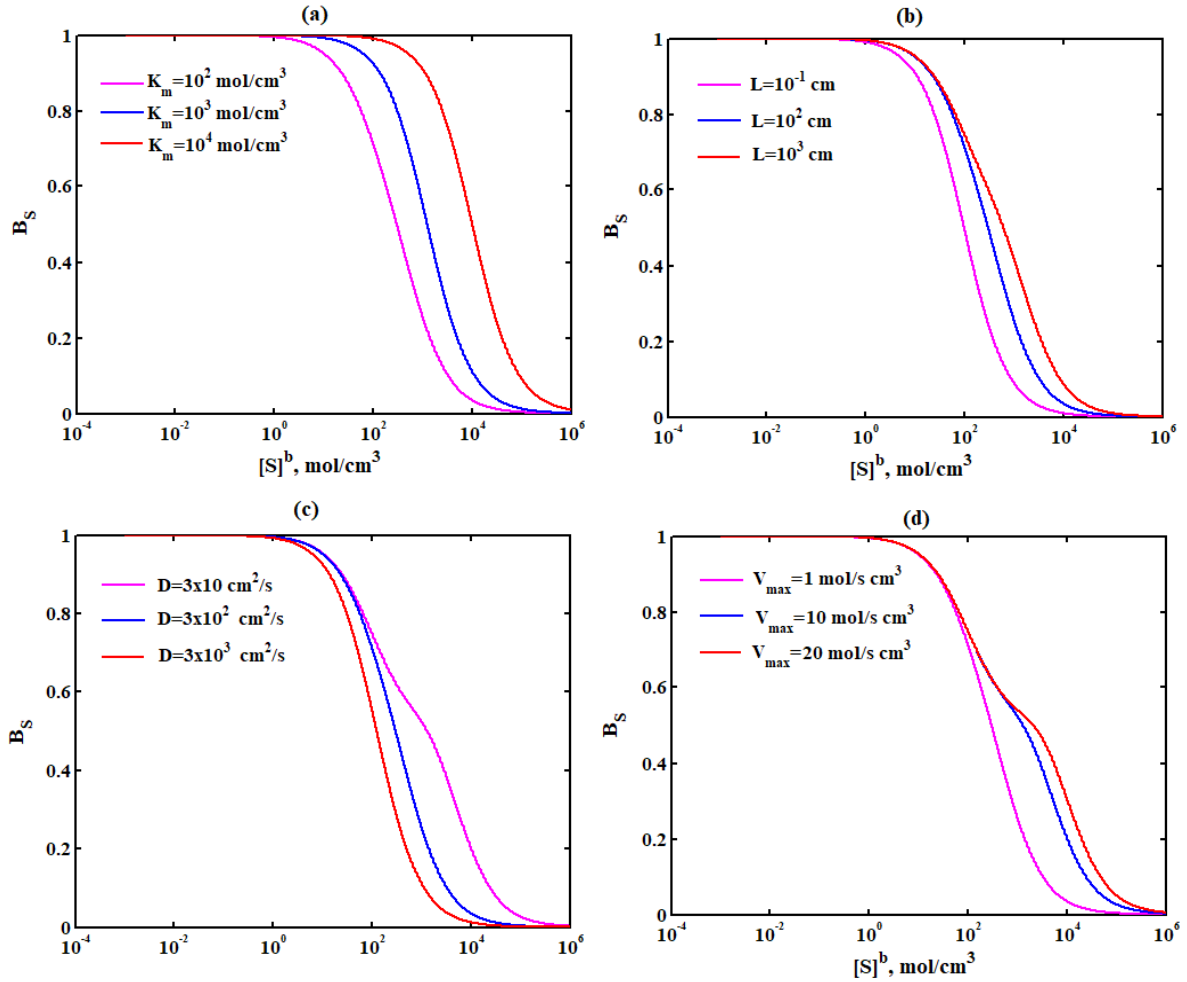

Figure 2. Biosensor sensitivity curve (Eq. (35)) given that (a) $D = 300\ \text{cm}^2/\text{s}, V_{\max} = 1\ \text{mol/s cm}^3, L = 500\ \text{cm}$ and various values of K_m, (b) $D = 300\ \text{cm}^2/\text{s}, V_{\max} = 1\ \text{mol/s cm}^3, K_m = 100\ \text{mol/cm}^3$ and various values of L, (c) $K_m = 100\ \text{mol/cm}^3, V_{\max} = 1\ mol/s\ cm^3, L = 500\ \text{cm}$ and various values of D, and (d) $D = 300\ \text{cm}^2/\text{s}, K_m = 100\ \text{mol/cm}^3, L = 500\ \text{cm}$ and various values of $V_{\max}$.

The biosensor sensitivity for different parameter values is displayed in Figure 2(a-d). From Figures 2(a, b, d), it is inferred that the biosensor sensitivity is proportional to the Michaelis-Menten constant, membrane thickness, and maximal enzymatic rate. Figure 2(c), on the other hand, shows the sensitivity is inversely proportional to the diffusion coefficient.

3.2. Resitance of biosensor

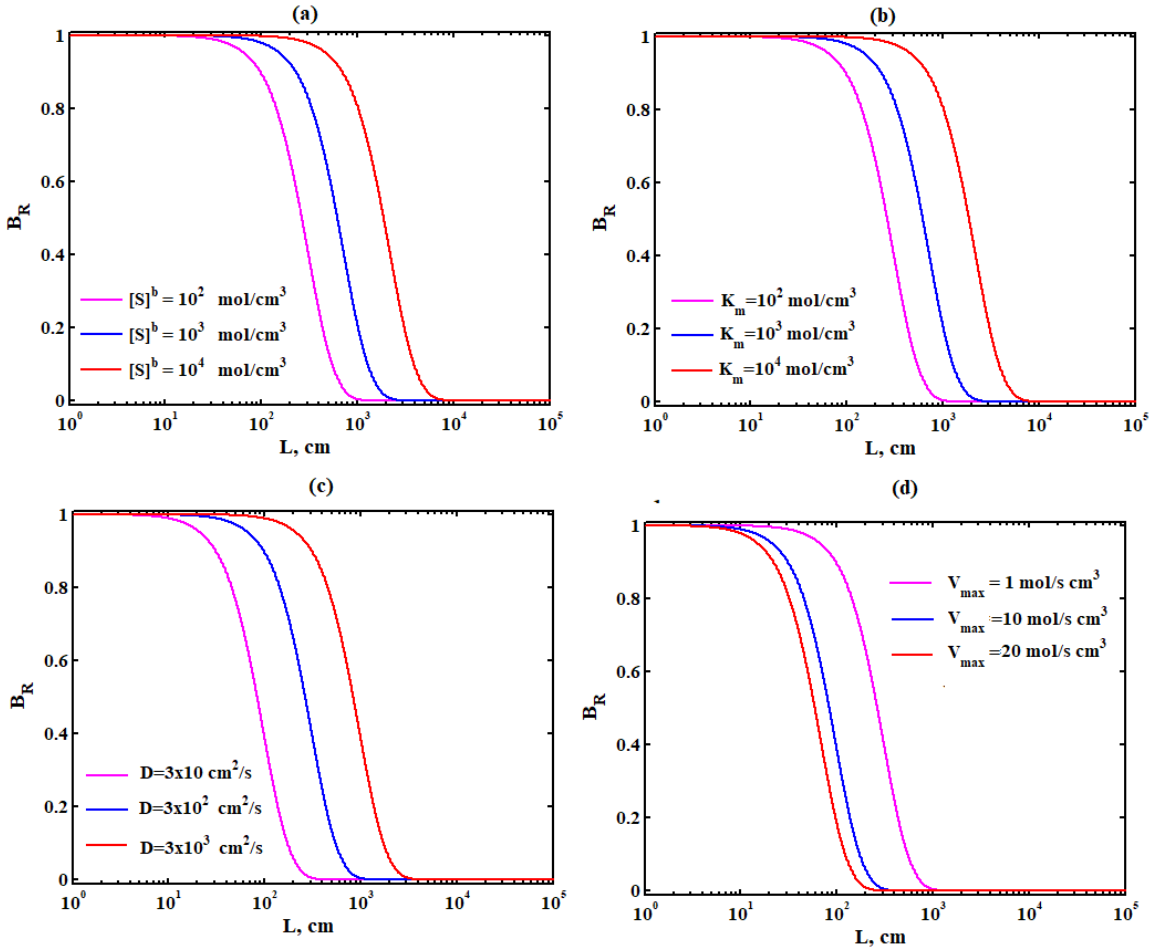

Figure 3. Biosensor sensitivity curve (Eq. (36)) given that (a) $D = 300\ \mathrm{cm}^2/\mathrm{s}, V_{\max} = 1\ \mathrm{mol/s\ cm}^3, K_m = 100\ \mathrm{mol/cm}^3$ and various values of $[S]^b$, (b) $D = 300\ \mathrm{cm}^2/\mathrm{s}, V_{\max} = 1\ \mathrm{mol/s\ cm}^3$, $[S]^b = \mathrm{mol/s\ cm}^3$ and various values of K_m, (c) $K_m = 100\ \mathrm{mol/cm}^3, V_{\max} = 1\ \mathrm{mol/s\ cm}^3, [S]^b = 100\ \mathrm{mol/s\ cm}^3$ and various values of D, and (d) $D = 300\ \mathrm{cm}^2/\mathrm{s}, K_m = 100\ \mathrm{mol/cm}^3, [S]^b = 100\ \mathrm{mol/s\ cm}^3$ and various values of $V_{\max}$.

In this section, we discuss the resistance of the membrane-based biosensors to the changes in thickness. The steady-state biosensor current gradient to the enzyme layer thickness L is the normalized dimensionless biosensor resistance B_R [45].

$$B_R(L) = \frac{L}{I(L)}\frac{\mathrm{d}I(L)}{\mathrm{d}L} = m(\coth(m) - \tanh(m)), \tag{35}$$

where $I(L)$ is the steady-state biosensor current calculated at the thickness of the enzyme layer L. From Eq. (36), it is observed that the resistance B_R varies between 0 and 1.

Figure 3(a-d) illustrates the biosensor resistance B_R versus the membrane thickness L for different values of the parameters. The normalized resistance curves' shapes conclude that an increase in the membrane thickness decreases resistivity. In other words, the maximal and the minimal biosensor resistance are directly proportional to Thiele's modulus.

Figure 3(a-c) confirms that an increase in the bulk concentration ($[S]^b$), Michaelis-Menten constant (K_m), or diffusion coefficient (D) lead to an increase in the resistance. In contrast, the increasing value of maximal enzymatic rate ($V_{\max}$) implies a decrease in resistance as portryed in Fig 3(d).

4. CONCLUSIONS

The Akbari-Ganji method was employed to derive simple semi-analytic approximate expressions of steady-state concentrations of organophosphorus pesticides (OPs) and deprotonation products for all possible values of parameters. In addition, approximate analytical expressions of the current at steady-state, the sensitivity, and resistance were also derived. The derived analytical expressions were employed to investigate the biosensor sensitivity and resistance to various parameters of the model.

APPENDIX A: Approximate analytical solution of nonlinear Eq. (15) using AGM method

Consider the differential equation (15):

$$F(\overline{x}) = \frac{d^2\,\overline{[\mathrm{S}]}}{d\overline{x}^2} - a^2\frac{\overline{[\mathrm{S}]}}{\overline{[\mathrm{S}]}+1} = 0, \tag{A.1}$$

with boundary conditions:

$$\frac{d\overline{[\mathrm{S}]}}{d\overline{x}}(0) = 0, \qquad \overline{[\mathrm{S}]}(1) = \overline{[\mathrm{S}]^{\mathrm{b}}}. \tag{A.2}$$

Assume that the solution of equations (A.1) is given by

$$\overline{[\mathrm{S}]}(\overline{x}) = A\cosh(m\overline{x}) + B\sinh(m\overline{x}), \tag{A.3}$$

where A, B, and m are constants to be determined.

From boundary condition (A.2), we readily obtain

$$A = \frac{\overline{[\mathrm{S}]}^b}{\cosh(m)}, \quad B = 0 \tag{A.4}$$

Replacing these constants into equations (A.3) gives

$$\overline{[\mathrm{S}]}(\overline{x}) = \overline{[\mathrm{S}]}^b\,\frac{\cosh(m\overline{x})}{\cosh m}, \tag{A.5}$$

where m is the constant coefficient.

Substituting the value of (A.5) into (A.1) implies

$$F(\overline{x}) = m^2\overline{[S]}^b \frac{\cosh(m\overline{x})}{\cosh m} - a^2 \frac{\cosh(m\overline{x})}{\cosh(m\overline{x}) + \cosh m} = 0, \quad \text{(A.6)}$$

and by substituting $\overline{x} = 1$ into (A.6), we get

$$F(\overline{x} = 1) = m^2\overline{[S]}^b - a^2 \frac{\overline{[S]}^b}{\overline{[S]}^b + 1} = 0. \quad \text{(A.7)}$$

From equation (A.7), the value of the constant m is obtained, that is

$$m = \frac{a}{\sqrt{1 + \overline{[S]}^b}}. \quad \text{(A.8)}$$

APPENDIX B MATLAB program to find the numerical solution of Eq. (15)

```
function pdex4
m=0;
x=linspace(0,1);
t=linspace(0,100000);
sol=pdepe(m,@pdex8pde,@pdex8ic,@pdex8bc,x,t);

u=sol(:,:,1);
figure
plot(x,u(end,:))
% .....................................................
function [c,f,s]=pdex8pde(x,t,u,DuDx)
c=1;
f =DuDx;
a = 0.1;
s = -(a^2*u)/(1+u);
% ,.....................................................
function u0=pdex8ic(x)
u0=0;
% .....................................................
function [p1,q1,pr,qr]=pdex8bc(x1,u1,xr,ur,t)
```

Sb=0.1;

p1=0;

q1=1;

pr = ur-Sb;

qr = 0;

NOMENCLATURE:

Symbol	**Definition**	**Usual units**
[S]	Substrate concentration	[mol/cm^3]
[P_hH]	Hydrolysis products of organo phosphodiester	[mol/cm^3]
[ZH]	Hydrolysis products of alcohol	[mol/cm^3]
[AH]	Added external buffer	[mol/cm^3]
P_h^-, Z^-, A^-, H^+	Deprotonation products	[mol/cm^3]
C_i	Concentration of the species	[mol/cm^3]
D_i	Diffusion coefficients	[cm^2/s]
R , r_{P_hH}, r_{ZH},r_{AH},r_{AH}	Rate of reactions	[μ mol/min]
k_1 , k_{-1}	Rate constant for the formation of the Michaelis complex	[cm/s]
k_2	Rate constant for the chemical transformation	[cm/s]
k_3	Rate constant for dissociation	[cm/s]
$[E]_t$	Enzyme concentration	[mol/cm^3]
$\overline{[S]}$	Dimensionless concentration of S	none
$\overline{[P_h]_T}$	Dimensionless concentration of P_hH	none
$\overline{[Z]_T}$	Dimensionless concentration of ZH	none
$\overline{[A]_T}$	Dimensionless concentration of AH	none
$\overline{[H^+]_T}$	Dimensionless concentration H^+	none
a	Thiele modulus	none
L	Thickness of membrane	[mol/s cm^3]
K_m	Michaelis-Menten constant.	[mol/cm^3]

K_{P_h}/K_m, K_Z/K_m,K_A/K_m	Equilibrium constants	none

References

1. W. Lihong, Z. Lin, H. Jinxing and C. Huanlin, *Chem. Eng. Technol*., 29 (2006) 462.
2. C. Ristori, C. Del Carlo, M. Martini, A.Barbaro and A. Ancarani, *Anal. Chim. Acta*, 325 (1996) 151.
3. N. Jaffrezic-Renault, *Sensors*., 1 (2001) 60.
4. A. Mulchandanietal, W. Chen, P. Mulchandani, J. Wang and K.R. Rogers, *Biosens. Bioelectron*., 16 (2001) 225.
5. K. R. Rogers, Y. Wang, A. Mulchandani, P. Mulchandani and W. Chen*, Biotech. Prog*., 15 (1999) 517.
6. D. P. Dumas, S. R. Caldwell, J. R. Wild and F. M. Raushel, *J. Biol. Chem*., 33 (1989) 19659.
7. D. P. Dumas, J. R. Wild and F. M. Raushel, *Biotechnol. Appl. Biochem*., 11 (1989) 235.
8. P. Mulchandani, A. Mulchandani, I. Kaneva and W. Chen, *Biosens. Bioelectron*., 14 (1999) 77.
9. A. Mulchandani, W. Chen, P. Mulchandani, J. Wang and K. R. Rogers, *Biosens. Bioelectron*., 16 (2001) 225.
10. P. Mulchandani, W. Chen, A. Mulchandani, J. Wang and L. Chen, *Biosens. Bioelectron*., 16 (2001) 433.
11. J. Wang, L. Chen, A. Mulchandani, P. Mulchandani and W. Chen, *Electroanalysis*, 11 (1999) 866.
12. J. Wang, M. P. Chatrathi, A. Mulchandani and W. Chen, *Anal. Chem*., 73 (2001) 1804.
13. D. H. Kim, G. S. Heo and D. W. Lee, *J. Chromatogr. Sci*. A, 824 (1998) 63.
14. A. Y. Kolosovaetal, *Anal. Chim. Acta*, 511 (2004) 323.
15. J. Sherma, *Anal. Chem.* 65 (1993) R40–R54.
16. S. D. Caras and J. Janata, *Anal. Chem*., 57 (1985) 1917.
17. S. Varanasi, R. L. Stevens and E. Ruckenstein, *AIChE J*., 33 (1987) 558.
18. A. Meena and L. Rajendran, *Chem. Eng. Technol*., 33 (2010) 1999.
19. J. Saranya and L. Rajendran, *Am. J. Analyt. Chem*., 7 (2016) 363.
20. K. Saravanakumar and L. Rajendran, *Appl. Math. Model*., 39 (2015) 7351.
21. H. Jafari and S. Seifi, Commun. *Nonlinear Sci*., 14 (2009) 2006.
22. J.H. He and F.Y. Ji, *J. Math. Chem*., 57 (2019) 1932.
23. M. Abukhaled, *J. Math.,* 2013 (2013) 720134.
24. M.C. Devi, P. Pirabaharan, L. Rajendran and M. Abukhaled, *Reac. Kinet. Mech. Cat*., 133 (2021) 655.
25. A. M. Wazwaz, A. *Appl. Math. Comput*., 102 (1999) 77.
26. M. Abukhaled and S. A. Khuri, *Int. J. Appl. Comput. Math*, 7 (2021) 1.
27. M.Abukhaled and S.A. Khuri, *Int. J. Comput. Methods Eng. Sci. Mech.*, 21 (2020) 159.
28. J. H. He, *Appl. Mech. Eng*., 178 (1999) 257.
29. R. Swaminathan, K. Lakshmi Narayanan, V. Mohan, K. Saranya and L. Rajendran, *Int. J. Electrochem. Sci.,* 14 (2019) 3777.
30. M.S.M Selvi, L. Rajendran, M. Abukhaled, *J. Marine. Sci. Appl*. 20 (2021) 55.
31. R. JoySalomi, S. Vinolyn Sylvia, L. Rajendran and M.E.G. Lyons, *J. Electroanal. Chem*., 895 (2021) 115421.
32. A.-M. Wazwaz, *Appl. Math. Comput*., 97 (1998) 37.
33. J.H. He, *Ain Shams Eng. J.,* 11 (2020) 1411.

34. S. Vinolyn Sylvia, R. Joy Salomi, L. Rajendran and M. Abukhaled, *Solid State Technol*., 63 (2020) 10090.
35. R. Swaminathan, M.C. Devi, L. Rajendran and K. Venugopal, *J. Electroanal. Chem*., 895 (2021) 115527.
36. R.U. Rani, L. Rajendran and MEG Lyons, *J. Electroanal. Chem*., 886 (2021) 115103.
37. M. R. Akbari, D. D. Ganji, A. Majidian, and A. R. Ahmadi, *Front. Mech. Eng*., 9 (2014) 177.
38. M. R. Akbari, D. D. Ganji, A. R. Goltabar, *Dev. Appl. Ocean. Eng*., 3 (2014) 22
39. B. Manimegalai, M. E. G. Lyon and L. Rajendran, *J. Electroanal. Chem*., 880 (2021) 114921.
40. J. Visuvasam, A. Meena and L. Rajendran, *J. Electroanal. Chem*., 869 (2020) 114106.
41. M. Mary, M.C. Devi, A. Meena, L. Rajendran and M. Abukhaled, *Reac. Kinet. Mech. Cat*., 134 (2021) 641.
42. K. Nirmala, B. Manimegalai, L. Rajendran, *Int. J. Electrochem. Sci*., 15 (2020) 5682.
43. R. Swaminathan, K.L. Narayanan, V. Mohan, K. Saranya and L. Rajendran, *Int. J. Electrochem. Sci.,* 14 (2019) 3777.
44. M. Kirthiga, S. Balamurugan, L. Rajendran, *Chem. Phys. Lett*., 715 (2019) 20.
45. R. Baronas, F. Ivanauskas and J. Kulys, Mathematical Modeling of Biosensors: An Introduction for Chemists and Mathematicians, Springer, (2010) Dordrecht, Netherlands.